STUDY ON STABILITY OF CONTROL SYSTEM FOR LARGE STROKE LINEAR MOTOR DRIVE PLATFORM

P. Ma*, Y.S. Ye, T.F. Deng, X.H. Wang, H.D. Zhao

In order to improve the steady-state tracking performance, system response speed and stability of the large stroke linear motor drive platform, the three closed-loop control system of the air flotation platform is designed. Firstly, the model is established based on the relevant parameters of the linear motor, and the stability of the current loop, the speed loop and the position loop is analyzed respectively. Secondly, based on feedforward control, a fuzzy feedforward control strategy is proposed to improve the system control performance under the premise that the system has sufficient stability margin. The simulation results show that the response speed of the system with fuzzy feedforward control is improved by 79.2%, and the steady-state tracking performance is improved by 85%.

Keywords: air floating platform, fuzzy feedforward control, stability, response speed, static accuracy

1 Introduction

With the development of manufacturing industry, the requirements for the response speed and trajectory tracking performance of large-stroke motion control platform are getting higher and higher. Large-stroke linear air-floating platform is a key component of high-speed and ultra-precision equipment. Its feed system is mostly driven by linear motor and air-floating support, which cancels the intermediate transmission link and improves the transmission efficiency and reliability [1]. However, due to its minimal friction damping and small electrical time constant, the control difficulty of linear servo system is increased. Stability is the prerequisite for the normal operation of the control system. The premise to improve the performance of the system should be to ensure that the system has sufficient stability margin. There is a certain research foundation for the stability of the servo control system in China and abroad. Reference [2] proposed a PID controller based on the model reference adaptive controller to overcome the shortcomings of the traditional PID controller that cannot solve the highly nonlinear system, and modified it based on the Lyapunov rule. The experiment verified that the controller effectively suppressed the system overshoot and better stability margin. Reference [3] analyzed the performance of the extended state

*College of Mechanical and Electrical Engineering, Guangdong University of Technology, Guangzhou 510006, China, E-mail: pingma@gdut.edu.cn

observer and the active disturbance rejection controller based on the Bode diagram and the root locus method in the frequency domain, and further explained the relationship between the stability range and the bandwidth. Reference [4] added the active disturbance rejection controller to the control system of permanent magnet synchronous linear motor. In the derivation process, the description function method was used to analyze the stability of the current loop under different current loop parameters, and suggestions for the selection of controller parameters were given. A linear/nonlinear active disturbance rejection switching control method is proposed in reference [5]. Aiming at the excessive restrictions based on Lyapunov stability theorem analysis, a stability analysis method based on robust Popov criterion is proposed. It is verified that the control method can make the system obtain better tracking and disturbance rejection ability. Considering the domestic and foreign scholars ' research on the stability of large-stroke motion platform is mostly based on Lyapunov theory for theoretical verification, but from mathematical modeling to simulation process is complex, few scholars analyze the stability and stability margin of the control system. At the same time, on this basis, it is more rare to carry out research on improving system control performance.

In the actual work of the moving platform, the control system is inevitably affected by many nonlinear disturbances, such as non-periodic noise. Scholars have many research results in improving the control performance of motion control system, but few scholars combine fuzzy control and feedforward control, and even apply fuzzy control algorithm to online debugging feedforward controller rather than classical PID controller. Fuzzy control does not require accurate mathematical model, which is suitable for solving the nonlinear and lag problems in process control, but simple information fuzzy processing may reduce the control accuracy. Feedforward control is based on the advance adjustment of disturbance, which can reproduce the input of system signal to the greatest extent, but the disturbance is mostly nonlinear and complex. In this paper, the two control strategies are combined complementarily, and a fuzzy feedforward control strategy based on feedforward control is proposed to ensure the stability margin of the control system and solve the problem that feedforward control is susceptible to nonlinear interference.

2 Characteristics of ultra-precision linear air float platform

The GD-V two-dimensional gantry precision air flotation platform studied by the research group consists of IMAC400 controller, IMAC DRIVE servo driver, two linear servo motors and corresponding accessories. The air flotation platform adopts the I-Force coreless 410 series of permanent magnet linear servo motor from PARK Company. This type of motor structure is bilateral, which can

eliminate the unilateral magnetic pull [6-7]. And the coreless motor does not have cogging effect, which means that compared with the same type of core motor, it has higher acceleration and mechanical bandwidth.

The overall structure of the moving platform is shown in Fig. 1. The air-bearing guide rails of the moving platform are all closed T-type air-bearing structures. This structure can constrain each degree of freedom except the moving direction of the platform. It has the characteristics of large bearing capacity, high stiffness and large overturning moment [8].

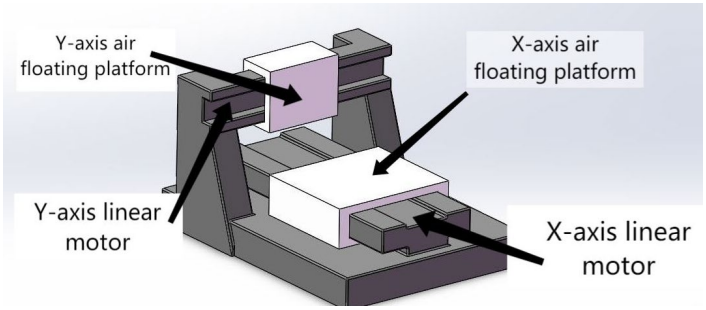

Fig. 1: Motion platform structure diagram

The maximum acceleration of the floating platform studied in this paper can reach 1G, and the measurement accuracy can reach 0.1, which has the characteristics of high speed, high precision and good stability. However, the sudden change of applied load in the actual working conditions will have a great impact on the stability and dynamic characteristics of the platform, and the research on it has certain engineering significance. Therefore, this paper will model the control system of the flotation platform according to the mechanism and conduct simulation research. The specific parameters of linear motor are shown in Table 1.

Table 1

Related parameters of linear motor

parameter	Sign(Unit)	X-axis	Y-axis
Armature inductor	$L(H)$	0.03	0.02
armature resistance	$R(\Omega)$	24	16
electrical time constant	$T_m(ms)$	1.25	1.25
Thrust constant	$K_f(N/A)$	163.7	109
quality	$M(kg)$	197.0	66.7
back electro-motive force	$\varepsilon(V/m/A)$	189	126
active radius	$S(mm)$	750	500
Peak thrust	$P(N)$	2967	2006

The main control mode of motor drive control system is three closed-loop control [9], which is composed of current loop, speed loop and position loop. According to the engineering design method, the current loop is designed and corrected first. Then the current loop is equivalent to an inertial link as part of the speed loop, and then the speed loop is corrected. Finally, the position loop is corrected. In this paper, according to the engineering design requirements [10], the stability margin determination index is established: amplitude margin Gm ≥ 10 dB, phase margin Pm ≥ 60°.

In this paper, the three closed-loops of the control system adopt PI regulator, which is mainly based on dynamic stability and response speed. A fuzzy control strategy based on feedforward control is proposed to comprehensively improve the response speed and steady-state accuracy under the premise of system stability. The control system structure is shown in Fig. 2, and the parameters in the figure can be referred to Table 1.

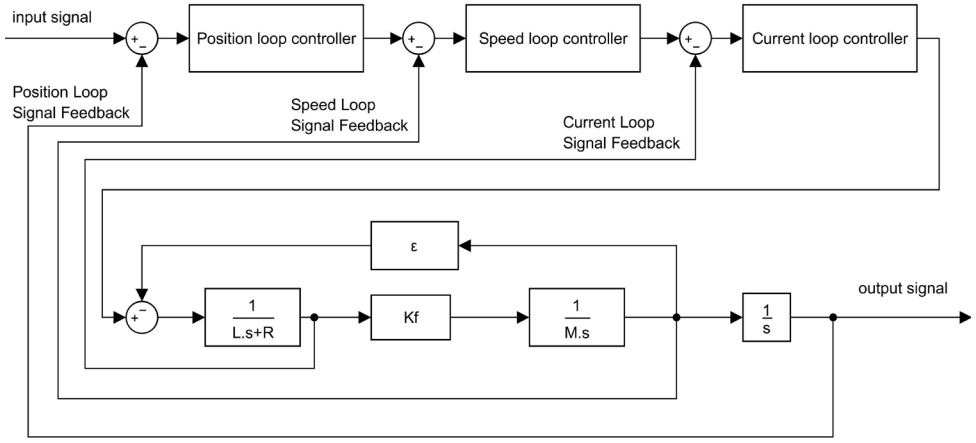

Fig. 2: Control system structure diagram

3 Characteristic Analysis of Linear Servo Control System

3.1 Current loop analysis

There are two main functions of the current loop controller. One is to enhance the ability of the system to resist power disturbance. The other is to regulate the current and limit the amplitude at the start and stop. It is mainly composed of current loop controller, PWM inverter, current amplifier and current rectifier filter. PWM inverter controls voltage output by con-trolling pulse width. Rectifier filter can eliminate interference in current feedback signal. The lag caused by the above two can be regarded as a small inertia link. Because the

electromagnetic inertia of linear motor winding is far less than the mechanical inertia, the influence of velocity back electromotive force on current loop can be ignored. In engineering design, the current loop is often designed according to the typical type I system [11]. The current loop structure is shown in Fig. 3.

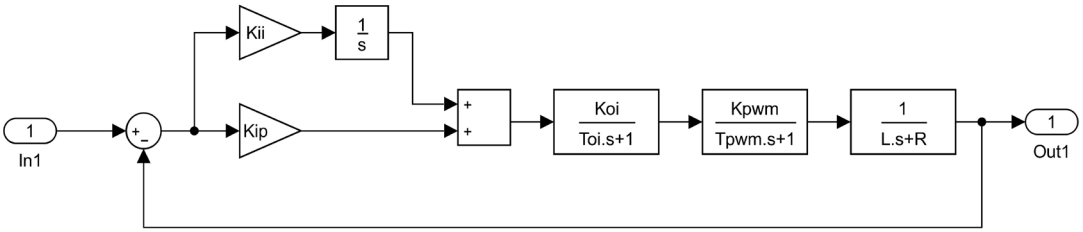

Fig. 3: Current loop structure diagram

According to the synthesis principle of small inertia link, the order reduction is carried out to establish the closed-loop transfer function and open-loop transfer function of the current loop:

$$G_{iB}(s) = \frac{1}{(\tau_{ii} / KK_i K_{ip})s + 1)} = \frac{1}{(T_i^{'} s + 1)} \tag{1}$$

$$G_i(s) = \frac{KK_{oi}K_{pwm}K_{ip}(\tau_{ii}s + 1)}{\tau_{ii}s(T_{oi}s + 1)(T_{pwm}s + 1)(T_m s + 1)} \tag{2}$$

Including:

$$K_{ii} = K_{ip} / \tau_{ii} \tag{3}$$

$$K^{'} = KK_i K_{ip} / \tau_{ii} \tag{4}$$

$$K = 1/R \tag{5}$$

$$K_i = K_{oi} / K_{pwm} \tag{6}$$

$$\tau_{ii} = T_m \tag{7}$$

$$T_{pwm} \approx 1/2f_{\Delta} \tag{8}$$

$$K_{pwm} = U_d / 2\sqrt{2}A_{\Delta} \tag{9}$$

$$T_i^{'} = 1/K^{'} \tag{10}$$

In the formula: τ_{ii} is the time integral constant(s); K_{ip} is the current loop proportional coefficient(V/A); K_{ii} is the current loop integral coefficient(V/A); T_{pwm} is the inverter time constant; K_{pwm} is the inverter amplification factor; K_{oi} is the current feedback filtering amplification coefficient; T_{oi} is the filter time constant(s); K_i control gain of small inertia link (V/A); T_{m} is the electrical time constant(s); f_{Δ} is the inverter triangular carrier frequency(KHZ); U_d is the DC bus

voltage of inverter(V); A_{Δ} is the triangular load amplitude of inverter(V); T_i' is the time constant of equivalent inertia link of current loop(s).

The values in the formula are shown in Table 2, in which the control gain of the small inertia link $K_i = K_{oi}K_{pwm} = 21.2$ V/A, Since the current loop is designed according to the typical type I system, and the controller zero is used to eliminate the large time constant poles of the control object, the electrical time constant $T_{\mathrm{m}} = L/R = 1.25$ ms is selected, and the equivalent inertia link coefficient of the cur-rent loop is taken, so the equivalent inertia link time constant of the current loop is $T_{\mathrm{i}}' = 1.49\times10^{-4}$ ms.

Table 2

Current loop parameters

Sign	Unit	Value
τ_{ii}	ms	1.25
T_{pwmX}	s	5×10^{-5}
T_{pwmY}	s	4.54×10^{-5}
K_{pwm}	-	21.2
K_{oi}	V/A	1
T_{oiX}	s	3.3×10^{-5}
T_{oiY}	s	3×10^{-5}
A_{Δ}	V	5
f_{Δ}	KHZ	11
U_d	V	200
K_i	V/A	21.2

According to the above parameters, the proportional coefficient K_{ipX}, K_{ipY} and integral coefficient K_{iiY}, K_{iiY} of X and Y axes are preliminarily debugged by MATLAB software, which are $8.949\,V/A$, $6.368\,V/A$, $7098\,V/A$ and $5268\,V/A$, respectively. The open-loop transfer function of the current loop of X and Y axes can be obtained from Eq. (2):

$$G_{iX}(s) = \frac{7.905}{1.25\times10^{-3}s(3.3\times10^{-5}s+1)(5.0\times10^{-5}s+1)} \tag{11}$$

$$G_{iY}(s) = \frac{8.438}{1.25\times10^{-3}s(3\times10^{-5}s+1)(4.54\times10^{-5}s+1)} \tag{12}$$

MATLAB simulation is used to analyze the open-loop transfer function of the current loops of X-axis and Y-axis linear motors in frequency domain. As shown in Fig. 4, it can be seen that the phase angle margin of the two axes is 62.4°

and 62.8°, and the amplitude margin is 18 dB and 18.3 dB, which meets the engineering design requirements.

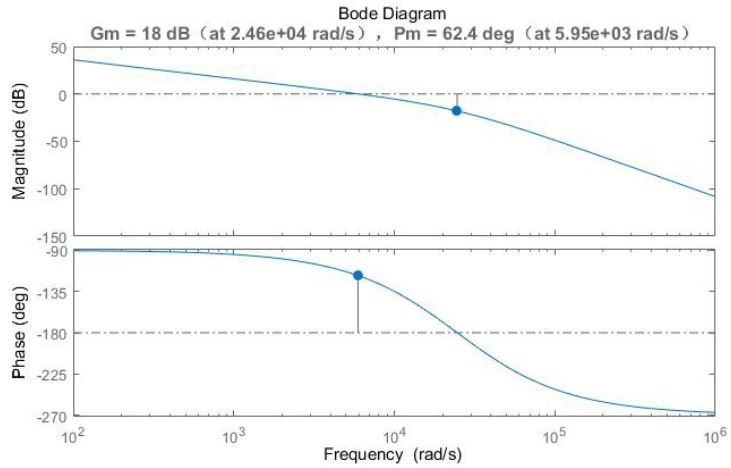

a) X-axis

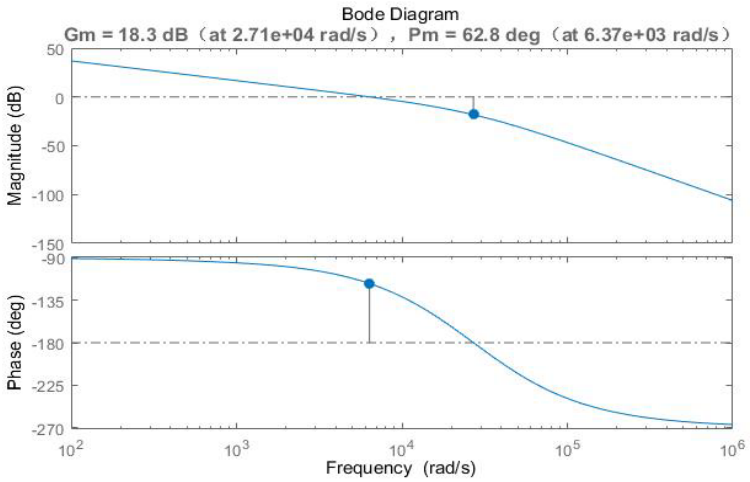

b) Y-axis

Fig. 4: Open loop Bode diagram of current loop

3.2 Speed loop analysis

The bandwidth and stability of the speed loop are of great significance for the dynamic performance and stability of the linear servo control system. The low-pass filtering link needs to be added to the system [12], and the low-pass filtering link will cause a certain amount of delay in the system. As the inner loop of the speed loop, the current loop is designed as an inertial link with the same time constant to balance the system delay. Therefore, in this paper, the current

loop is equivalent to the inertial link of the time constant s, and the structure of the speed loop is shown in Fig. 5.

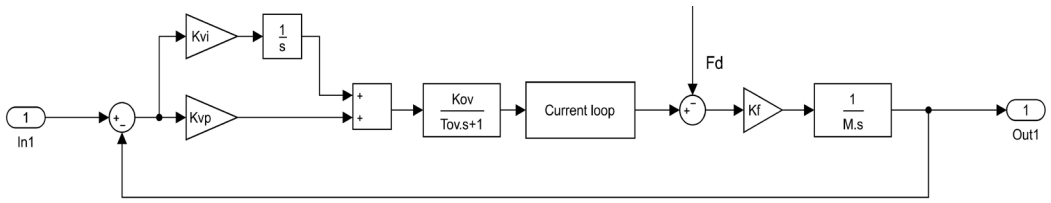

Fig. 5: Velocity loop structure diagram

As shown in Fig. 5 and Eq. (1) above, the open loop transfer function of the velocity loop is:

$$G_v(s)=\frac{K_{vp}(T_{vi}s+1)K_{ov}K_f}{T_{vi}s(T_{ov}s+1)(T_i's+1)Ms} \tag{13}$$

$$G_v(s)=\frac{\frac{K_{vp}K_{ov}K_f}{T_{vi}M}(T_{vi}s+1)}{s^2(T_{ov}s+1)(T_i's+1)} \tag{14}$$

In the formula: K_{vp} is the proportional coefficient of velocity loop (V/A); T_{vi} is the velocity loop integral time constant(s); K_{ov} is the speed feedback filter amplification factor; T_{ov} is the time constant of velocity filtering(s).

Speed Feedback Filter Amplification Coefficient Based on Servo Motion Controller Parameters: $K_{ovX}=53.5$, $K_{ovY}=57.2$, $T_{ov}=1ms$. According to the typical type II system to design the speed loop [13], the corresponding open-loop transfer function $K_{II}(\tau_{ii}s+1)/s^2(T_{II}s+1)$ and Eq.(14) are compared, $K_{II}=K_{vp}K_{ov}K_f/T_{vi}M$, $T_{II}=T_{ov}+T_i'$, $\tau_{II}=T_{vi}$. The typical type II system defines h as the width of the mid-frequency band, and the mid-frequency width coefficient $h=\tau_{II}/T_{II}$ to the attenuation oscillation property of the system, the comprehensive cost performance ratio of $h=5$ is the highest [14]. At this moment, time integral constant $\tau_{II}=h(T_{ov}+T_i')=5.745\times10^{-3}s$, $K_{II}=(h+1)/2h^2T_{II}{}^2=90895.25$. Therefore, it can be judged that the proportional coefficients of velocity loop of two axes are $K_{vpX}=K_{II}T_{vi}M/K_{ov}K_f=11.746As/mm$, $K_{vpY}=K_{II}T_{vi}M/K_{ov}K_f=5.586As/mm$, and the integral coefficients of velocity loop of two axes are $K_{viX}=K_{vpX}/T_{vi}=2044.56As/mm$, $K_{viY}=K_{vpY}/T_{vi}=972.32As/mm$, so the transfer function of velocity loop is:

$$G_{vX}(s)=\frac{522.19\times(s+174.06)}{s^2(1\times10^{-3}s+1)(1.49\times10^{-4}s+1)} \tag{15}$$

$$G_{vY}(s)=\frac{522.15\times(s+174.06)}{s^2(1\times10^{-3}s+1)(1.49\times10^{-4}s+1)} \tag{16}$$

The open-loop transfer function of velocity loop is analyzed in frequency domain, and Fig. 6. It can be seen from the figure that the amplitude margin of X and Y axes is 21.4 dB, and the phase margin is 40.1°, which does not meet the requirements of engineering design.

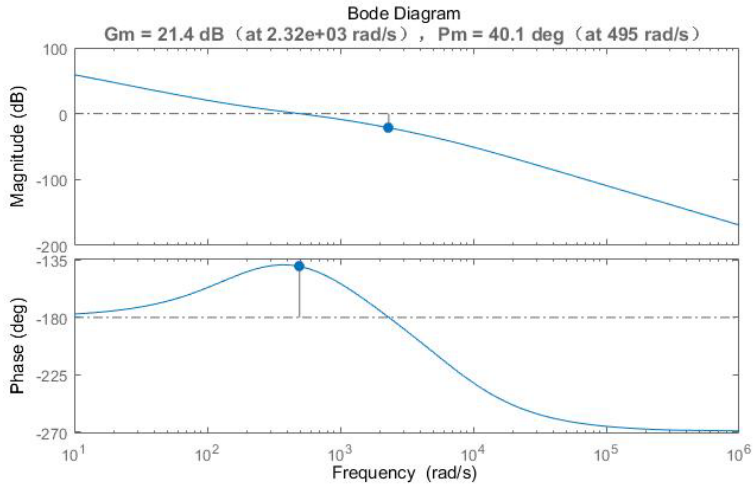

Fig. 6: Bode diagram of velocity loop (before correction)

Since the linear servo system is directly affected by the interference force without buffer, and the air-floating support is used to make the system damping too small, sufficient stability margin is needed to maintain the stability of the system. Therefore, the speed loop transfer function is calibrated. In this paper, the PID correction method is adopted. According to the requirements of engineering design performance, the appropriate proportional and integral coefficients are selected to improve the stability margin of the speed loop, and then the transfer function of the speed loop is approximated. The following is the open-loop transfer function of the corrected speed loop:

$$G_{vX}(s) = \frac{435.67(s+24)}{s^2(1\times10^{-3}s+1)(1.49\times10^{-4}s+1)} \tag{17}$$

$$G_{vY}(s) = \frac{448.68(s+25)}{s^2(1\times10^{-3}s+1)(1.49\times10^{-4}s+1)} \tag{18}$$

The frequency characteristics of the corrected speed loop are shown in Fig. 7. The amplitude margin of X and Y axis is 24.7 dB and 24.5 dB, and the phase margin is 61.2° and 60.5°, which meet the engineering design requirements.

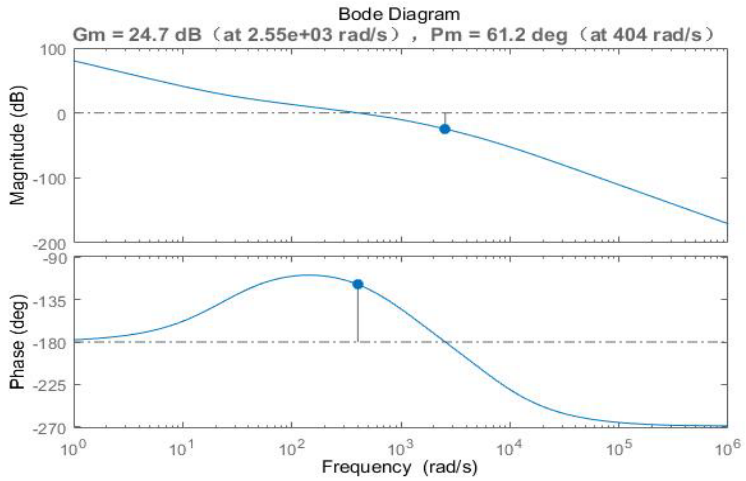

a) X-axis

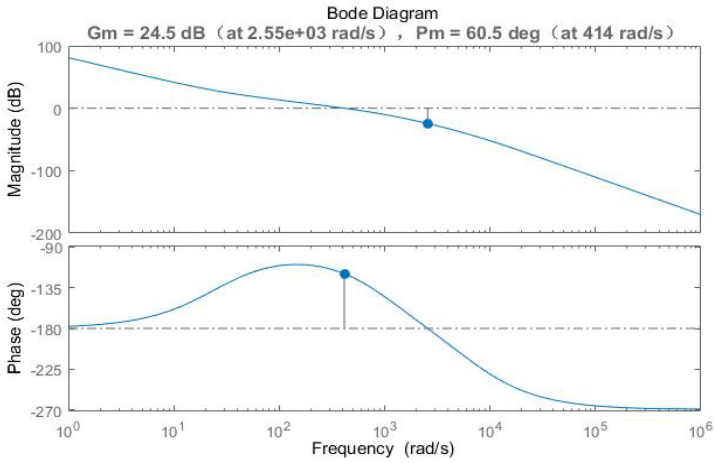

b) Y-axis

Fig. 7: Bode diagram of velocity loop (after correction)

3.3 Position loop analysis

The velocity ring is the inner ring of the position ring, which can be simplified as a link of the position ring. Fig. 8 is the structure of the position ring.

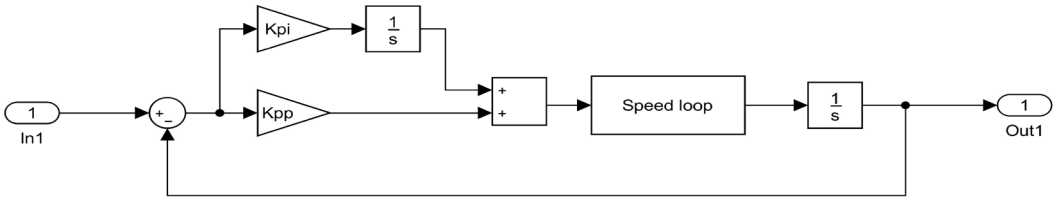

Fig. 8: Position loop structure diagram

From Fig. 8, the open loop transfer function of the position loop is:

$$G_p(s) = (K_{pp} + \frac{K_{pi}}{s}) \cdot \Phi_v \cdot \frac{1}{s} \tag{19}$$

The speed loop closed-loop transfer function:

$$\Phi_v = \frac{G_v(s)}{1 + G_v(s)} \tag{20}$$

The open loop transfer function of the position ring is obtained by Eq. (17) to (20):

$$G_{pX}(s) = \frac{(K_{ppX}s + K_{piX}) \cdot 435.67(s+24)}{[s^2(1\times10^{-3}s+1)(1.49\times10^{-4}s+1) + 435.67(s+24)] \cdot s} \tag{21}$$

$$G_{pY}(s) = \frac{(K_{ppY}s + K_{piY}) \cdot 448.68(s+25)}{[s^2(1\times10^{-3}s+1)(1.49\times10^{-4}s+1) + 448.68(s+25)] \cdot s} \tag{22}$$

In the formula: K_{pp} is the Proportional coefficient of position loop $(mm/s/mm)$, K_{pi} is the Integral coefficient of position loop (s^{-1}).

MATLAB software is used to debug the ratio and integral coefficient of position loop, according to Gm ≥ 10dB, Pm ≥ 60°, take $K_{ppX} = 100mm/s/mm$, $K_{piX} = 8s^{-1}$, $K_{ppY} = 130mm/s/mm$, $K_{piY} = 9s^{-1}$. The frequency domain analysis of the position loop of the two axes is shown in Fig. 9. The amplitude margin of the two axes are 17.8 dB and 11.5 dB, and the phase margin is 74.7° and 73.9°, meeting the requirements of engineering design.

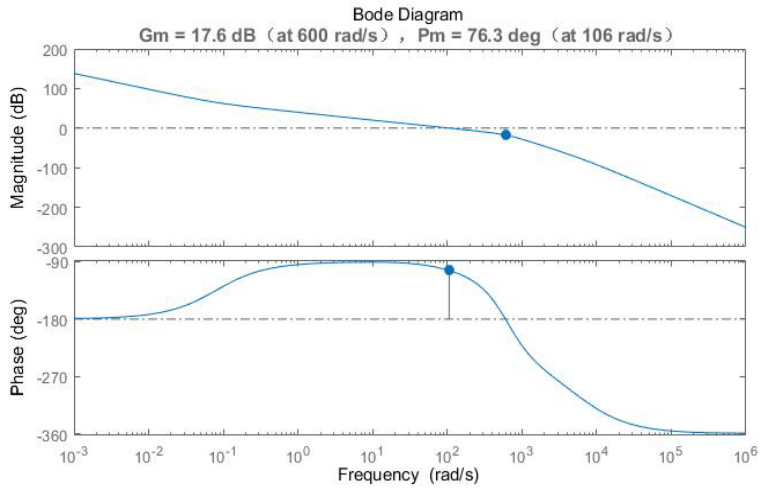

a) X-axis

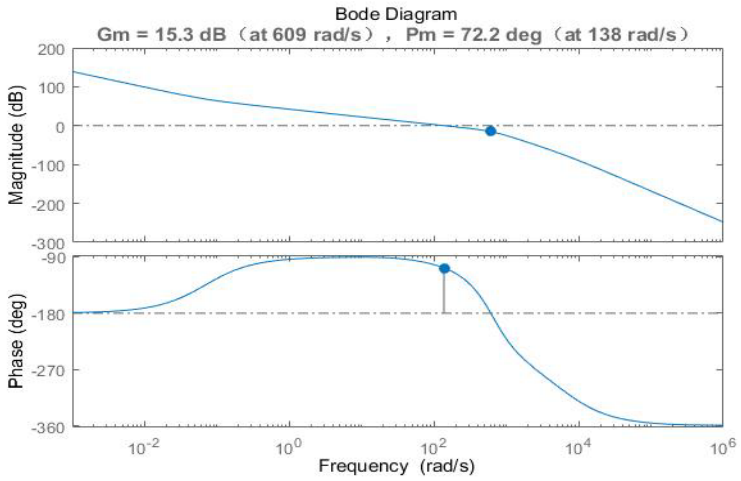

b) Y-axis

Fig. 9: Bode diagram of position loop

3.4 Design and comparative analysis of fuzzy feedforward controller

3.4.1 Fuzzy feedforward controller

The essence of the traditional PID feedback control is to eliminate the error by using the error between the target value and the actual value [15]. However, the target value is given outside the system and can be jumped. The actual value of the system output has a certain inertia, and it is impossible to jump. This is also the main reason why the PID control has the contradiction between rapidity and overshoot, when the controlled object is in a complex environment with constant changes.

According to the invariance principle [16], the introduction of feedforward control in the control system can speed up the system signal reproduction. However, the air-floating platform studied in this paper has the characteristics of large mass and sensitive to external disturbances. When the feedforward gain exceeds the effective parameter range or the parameters of the controlled object change, the stability margin of the control system cannot be guaranteed. In view of the above problems, a fuzzy control method based on feedforward control is proposed, and the feedforward gain is adjusted online, which not only ensures sufficient stability margin, but also improves the control performance of the system.

The system block diagram of the fuzzy controller is shown in Fig. 10. The position deviation e and its change rate ec of the control system are used as the input signals to output the feedforward increment, which is superimposed with the

initial value. Under the premise of system stability, the response speed and steady-state accuracy of the system are improved.

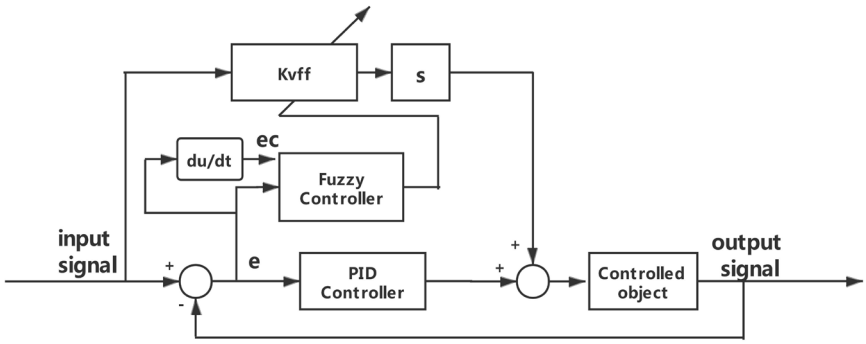

Fig. 10: Block diagram of fuzzy control system

In the fuzzy controller, the variation range of e is (-0.04, 0.04) mm, the variation range of ec is (-0.16, 0.16) mm/s, and the variation range of ΔK_{vff} is (-0.005, 0.005). In fuzzy rules, e, ec and ΔK_{vff} are taken as linguistic variables and NB (negative large), NS (negative small), ZO (zero), PS (positive small), PB (positive small) are taken as fuzzy subsets. The corresponding fuzzy universe is taken as {-1, -0.5, 0, 0.5, 1}, and e, ec and the ΔK_{vff} are all Gaussian membership function, as shown in Fig. 11.

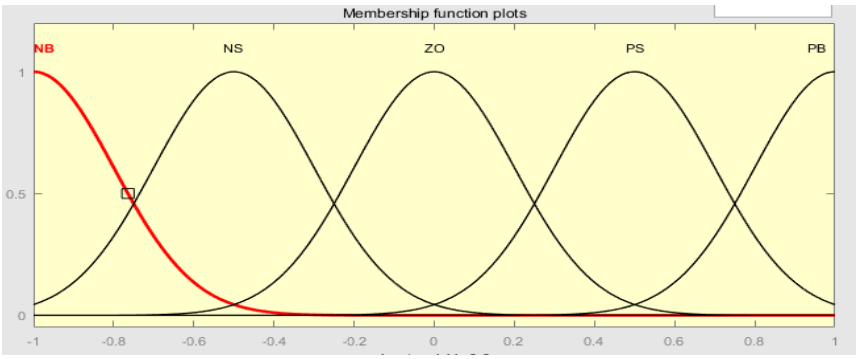

Fig. 11: Membership function curves

Fuzzy reasoning method uses Mamdani reasoning method, the specific fuzzy rules are shown in Tab. 3 below. Taking into account the complexity of the motion platform system, the gravity center method is selected to defuzzify it, and the output surface observer of ΔK_{vff} is obtained after defuzzification, as shown in Fig. 12.

Table 3

Fuzzy rule of K_{vff}

e ec	NB	NS	ZO	PS	PB
NB	PB	PB	PS	NB	PB
NS	PS	PS	PS	NS	PS
ZO	PS	PS	ZO	NS	PS
PS	PS	PS	PS	NS	PS
PB	PS	PB	PS	NB	PB

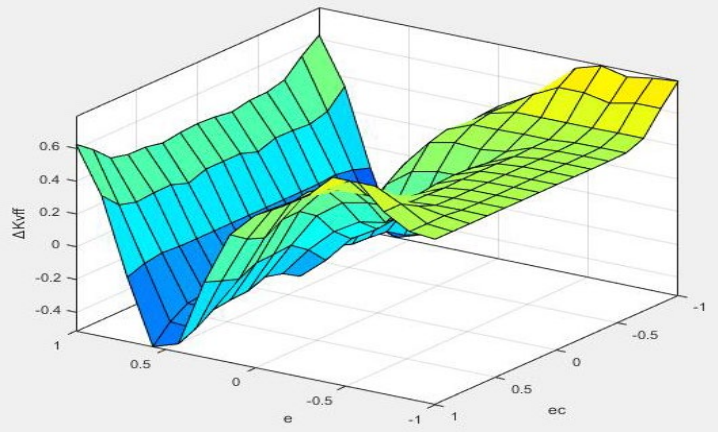

Fig. 12: Output Surface Observer

3.4.2 Comparative Analysis of Different Control Strategies

The fuzzy feedforward PID control, feedforward PID control and traditional PID feedback control are compared. The steady-state accuracy of the system is taken as the evaluation index. The input excitation signal of the position loop of the control system is a unit sinusoidal response with frequency of 4rad/s. The three pairs are shown in Fig. 13 below. It shows that the steady-state accuracy of the traditional PID feedback control is 0.04mm, 0.008mm after adding the feedforward control, and 0.006mm after adding the fuzzy feedforward control. The steady-state accuracy increases by 80% and 85%.

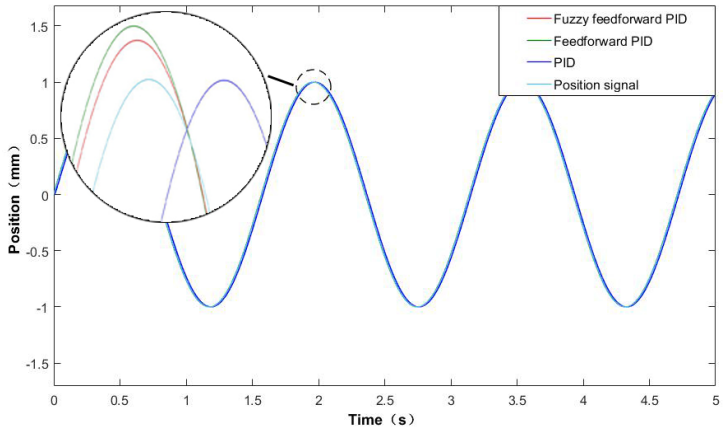

a) Sine response diagram

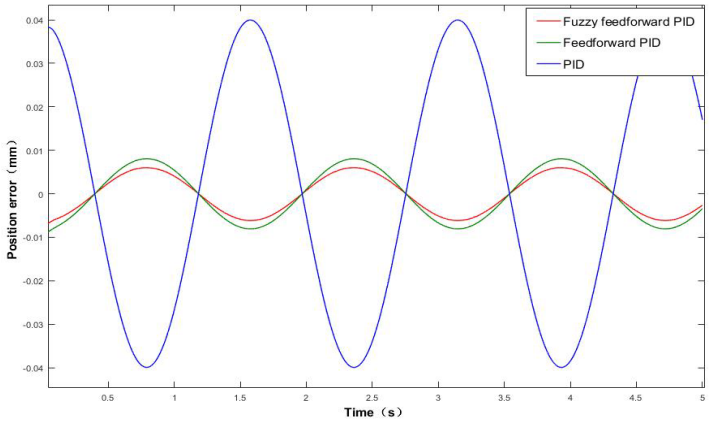

b) Error comparison diagram

Fig. 13: Comparison diagram of steady-state accuracy

Taking the response speed as the evaluation index, the unit square wave signal with the input frequency of 4rad/s in the position loop of the control system is compared and analyzed, as shown in Fig. 14. It shows that the rise time of traditional PID feedback control is 14.979ms. After adding feedforward control, it is 3.265ms, and the response speed increases by 78.2%. After adding fuzzy feedforward control, it is 3.118ms, and the response speed increases by 79.2%. And because of the square wave signal velocity direction mutation, so for feedforward control, fuzzy feedforward control two response speed good control mode, may have a large overshoot in a very short time, but in the system can withstand the overshoot range.

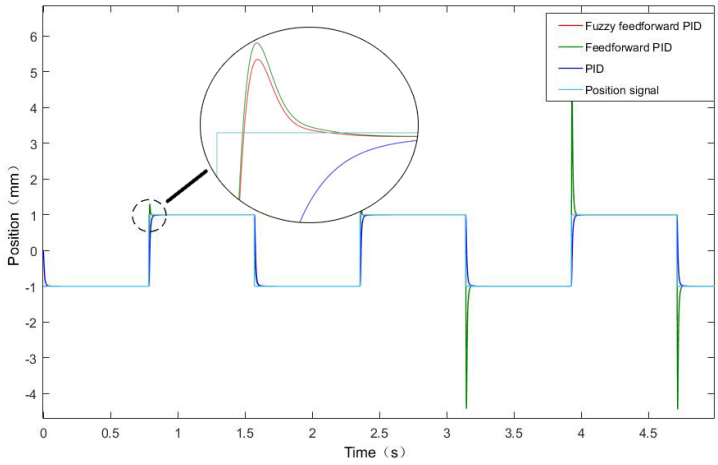

Fig. 14: Response speed comparison chart

Then the zero-pole diagram of the position closed-loop system is made, and it is found that after adding fuzzy feedforward control, the characteristic equation of the system can refer to the zero-pole diagram of Fig. 15, and the poles are all in the left half plane of the S plane, indicating that the system is in a stable state.

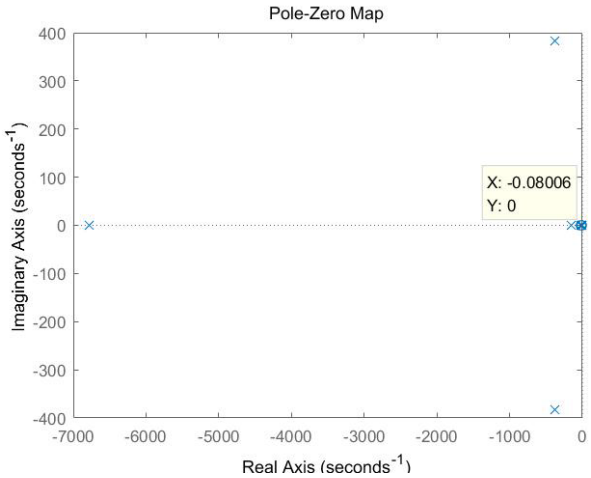

Fig. 15: Zero-pole map of position closed loop

4 Conclusion

In this article, the stability of the control system of the two-dimensional ultra-precision air flotation platform is studied. Based on the engineering design index of the actual working conditions, it is ensured that it has sufficient stability margin. Then, the control algorithm is added to the position loop to improve the

control performance of the servo control system. This study makes two contributions to the current scholarly literature.

Firstly, according to the specific equipment in the laboratory, the mathematical model is established for simulation analysis. In the derivation process, the frequency domain analysis of the control system is added, and the parameters are corrected to obtain the relationship between the controller parameters, stability margin and bandwidth. In the existing theories, most scholars' research methods are shown in Reference [5]. The excessive complexity of the theory cannot be compatible with the actual production, while the method in this paper is simple to implement in engineering and has practical significance in engineering.

Secondly, A fuzzy feedforward control strategy is proposed by complementing the robustness of fuzzy control and invariance of feedforward control. For these two control strategies, most of the existing theories have applied them to the traditional PID controller. In this paper, the fuzzy controller is applied to the output gain parameters of the online debugging feedforward control. In the early stage, the fuzzy inference rules are also partially modified according to the actual demand. In the simulation analysis process, the control performance of the three control strategies is compared. After the fuzzy feedforward control algorithm is added, the response speed of the system increases by 79.2 % and the steady-state accuracy increases by 85 %. Finally, the zero pole diagram of the closed loop position loop of the control system is analyzed, and the system is still in a stable state. Since the fuzzy control method has been widely accepted by the market, it shows that the fuzzy feedforward control strategy can not only be applied to the laboratory research and teaching work, but also has certain engineering practical significance.

Acknowledgement

This work was financially supported by Guangdong Key Area R & D Program (Project No. 2019B090918002).

REFERENCES

[1] *Zhang Bolin, Huang Xiaoming, Fan Mengwu,* Development trend of high speed machine tool feed system. Modular Machine Tool & Automatic Manufacturing Technique, (10): 9-13, 2002.

[2] *Mani G., Sivaraman N. and Kannan R.,* Visual Servoing Based Model Reference Adaptive Control with Lyapunov Rule for a Ball on Plate Balancing System. 2018 International Conference on Intelligent and Advanced System (ICIAS), pp. 1-6, 2018. doi: 10.1109/ICIAS.2018.8540635.

[3] *Zhang Dongyang, Wu Qinghe, and Yao Xiaolan,* Bandwidth Based Stability Analysis of Active Disturbance Rejection Control for Nonlinear Uncertain Systems. Journal of Systems

Science and Complexity, 31 (6): 1449-1468, 2018. https://doi.org/10.1007/s11424-018-7073-4

[4] *Zeng Yuenan, Zeng Xiangcai, Zhou Bin,* Nonlinear Active Disturbance Rejection Controller Design for Current Loop of PMSM Drive System and Its Stability Analysis. Transactions of China Electrotechnical Society, 32(17): 135-143, 2017. DOI: 10.19595/j.cnki.1000-6753.tces.160614

[5] *Li Jie, Qi Xiaohui, Xia Yuanqing, Gao Zhiqiang,* On Linear/Nonlinear Active Disturbance Rejection Switching Control. Acta Automatica Sinica, 42(2): 202-212, 2016. DOI: 10.16383/j.aas.2016.c150338

[6] *Sung-An Kim, Yu-Wu Zhu, Sang-Geon Lee, Subrato Saha, Yun-Hyun Cho,* Electromagnetic Normal Force Characteristics of a Permanent Magnet Linear Synchronous Motor with Double Primary Side. IEEE Transactions on Magnetics, vol. 50, no. 1, pp. 1-4, 2014. doi: 10.1109/TMAG.2013.2278397.

[7] *Chang-Eob Kim, Seong-Ho Lee, Dong-Hee Lee, Houng-Joong Kim,* The Analysis of Permanent Magnet Double-Sided Linear Synchronous Motor With Perpendicular Arrangement. IEEE Transactions on Magnetics, vol. 49, no. 5, pp. 2267-2270, 2013. doi: 10.1109/TMAG.2013.2244862.

[8] *Mo Deyun, Ma Ping, Gong Manfeng,* The Effects of the Interface Structure Fit on the Aerostatic Guideway Performance of T-Type Air Bearing Table. Machinery Design & Manufacture, 7(7), 211-214, 2015. DOI：10.19356/j.cnki.1001-3997.2015.07.058

[9] *Ang K.H., Chong G., Li Y.,* PID control system analysis, design, and technology. IEEE Transactions on Control Systems Technology, vol. 13, no. 4, pp. 559-576, 2005. doi: 10.1109/TCST.2005.847331.

[10] *Zhu Xiaogang, Ma Ping,* The Research of Control System Stability of Two-Dimensional Precision Areostatic Bearing Stage. Machinery Design & Manufacture, (08): 136-139, 2017. DOI: 10.19356/j.cnki.1001-3997.2017.08.039

[11] *Su Pingang, Shang Li,* Simulink simulation of double-closed loop DC speed regulation system with reversible PWM control. Experimental Technology and Management, 35(02): 124-129, 2018. DOI：10.16791/j.cnki.sjg.2018.02.030

[12] *Li J., Tsao T.C.,* Robust performance repetitive control systems. Journal of Dynamic Systems Measurement & Control, 123(3), 330-337, 2001. https://doi.org/10.1115/1.1387015

[13] *Dai Weili, Zhang Xiaofeng,* Compound Control of Variable Structure and Feedforward for Permanent Magnet Synchronous Servo Motor. Science Technology and Engineering, 19(04): 131-137, 2019.

[14] *Chen Boshi, Ruan Yi,* Automatic control system of electric drive: motion control system. Beijing: Mechanical Industry Press. 2010.

[15] *Ma Yantong, Zheng Rong, Yu Chuang,* Autonomous underwater vehicle deepening control based on transiting target value nonlinear PID. Control Theory & Applications, 35(08), 1120-1125, 2018.

[16] *Bu Wenshao, Tu Xiaowan, Lu Chunxiao, Pu Yi,* Adaptive feedforward vibration compensation control strategy of bearingless induction motor. International Journal of Applied Electromagnetics and Mechanics, 63(2): 199-215, 2020. DOI: 10.3233/JAE-190092